Supporting Information for

Rapidly characterizing the fast dynamics of RNA genetic circuitry with cell-free transcription-translation (TX-TL) systems

Melissa K. Takahashi[1,2], James Chappell[1], Clarmyra A. Hayes[3], Zachary Z. Sun[3], Jongmin Kim[3], Vipul Singhal[2,3], Kevin J. Spring[2,4], Shaima Al-Khabouri[2,5], Christopher P. Fall[2,6,7], Vincent Noireaux[8], Richard M. Murray[2,3], Julius B. Lucks[1,2]*

1 – School of Chemical and Biomolecular Engineering, Cornell University, Ithaca NY 14850
2 – CSHL Course in Synthetic Biology, Cold Spring Harbor Laboratory, Cold Spring Harbor, NY 11724
3 – Division of Biology and Biological Engineering, California Institute of Technology, Pasadena, CA 91125
4 – Department of Integrative Biology and Pharmacology, The University of Texas Medical School at Houston, TX 77030
5 – Institute for Research in Immunology and Cancer (IRIC), Universite´ de Montreal, Montreal, Quebec H3T 1J4, Canada
6 – Department of BioEngineering, University of Illinois, Chicago, IL 60607
7 – Department of Computer Science, Georgetown University, Washington, DC 20057
8 – School of Physics and Astronomy, University of Minnesota, Minneapolis, MN 55455

Appendix 1	Estimation of the Response Time of a Double-Inversion RNA Cascade	

Materials and Methods

Steady state *in vivo* gene expression

Plasmid combinations were transformed into chemically competent *E. coli* TG1 cells, plated on Difco LB+Agar plates containing 100 μg/mL carbenicillin, 34 μg/mL chloramphenicol, and 100 μg/mL kanamycin and incubated overnight at 37°C. Plates were taken out of the incubator and left at room temperature for approximately 7 h. Four colonies were used to inoculate 300 μL of LB containing carbenicillin, chloramphenicol, and kanamycin at the concentrations above in a 2 mL 96-well block (Costar 3960), and grown approximately 17 h overnight at 37°C at 1,000 rpm in a Labnet Vortemp 56 bench top shaker. 4 μL of this overnight culture were then added to 196 μL (1:50 dilution) of M9 minimal media containing the selective antibiotics and grown for 4 h at the same conditions as the overnight culture. 100 μL of this culture were then transferred to a 96-well plate (Costar 3631) containing 100 μL of PBS. SFGFP fluorescence (485 nm excitation, 520 nm emission) and optical density (OD, 600 nm) were then measured using a Biotek SynergyH1m plate reader.

RNA degradation in TX-TL

TX-TL buffer and extract tubes were thawed on ice for approximately 20 min. 2.2 μM of purified malachite green aptamer RNA was added to reaction tubes. Buffer and extract were mixed together with malachite green dye (Sigma M9015, final concentration 10 μM) and then added to the reaction tubes according to the previously published protocol [1]. 10 μL of each TX-TL reaction mixture was transferred to a 384-well plate (Nunc 142761), covered with a plate seal (Nunc 232701), and placed on a Biotek SynergyH1m plate reader. Temperature was controlled at either 29°C or 37°C. Malachite green fluorescence was measured (610 nm excitation, 650 emission) every 30 seconds. Fluorescence trajectories were fit to an exponential decay function in the form of $y(t) = a*\exp(-t/\tau) + b$. Fitted values of τ were used to calculate the half life ($t_{1/2}$) of the malachite green aptamer in TX-TL.

Supporting Figures and Tables

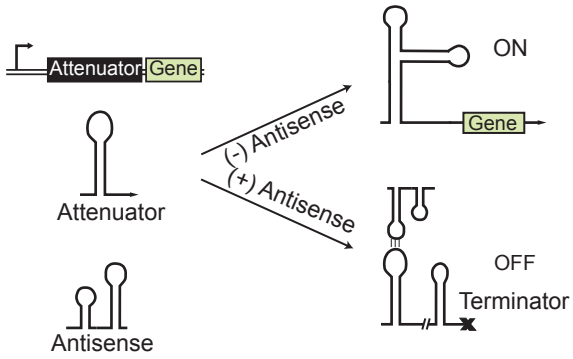

Figure S1. The transcriptional attenuation mechanism from the *Staphylococcus aureus* plasmid pT181[2,3]. The attenuator lies in the 5' untranslated region of the transcript and can fold into a structure that will allow transcription to continue if antisense RNA is not present (ON). Antisense RNA binding to the attenuator causes the formation of a

terminator hairpin, stopping transcription before the gene of interest (OFF, indicated by x symbol). Figure modified from Takahashi and Lucks[4].

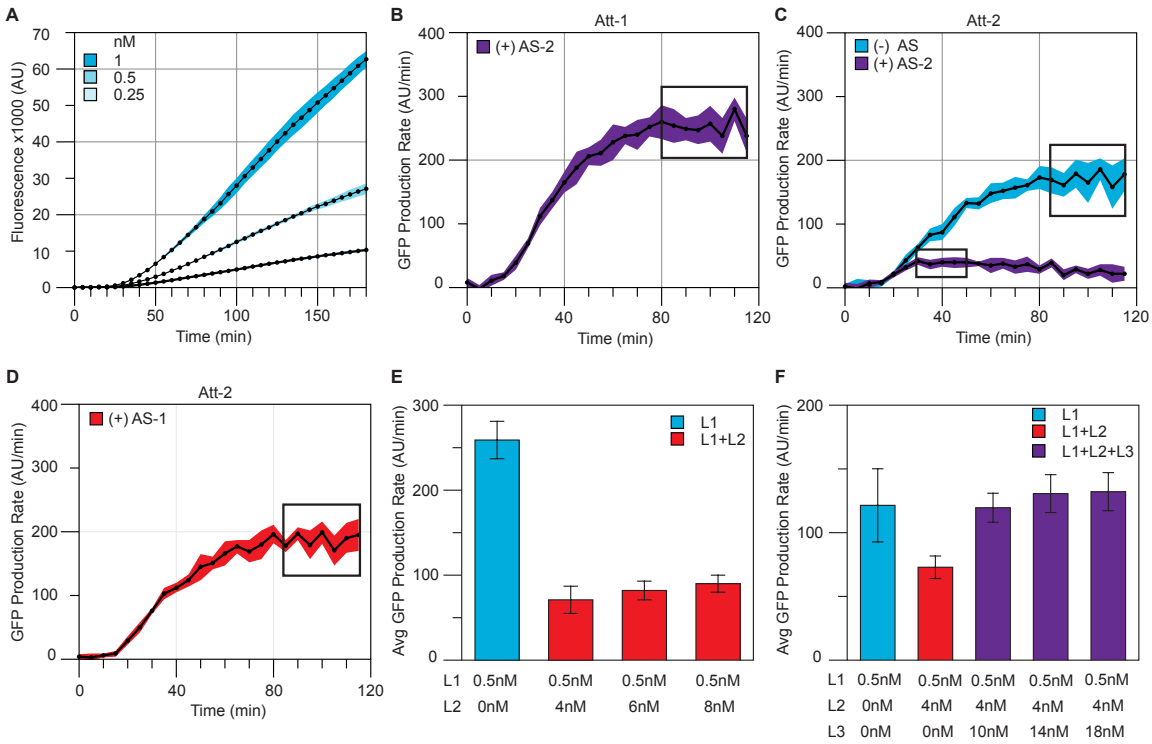

Figure S2. (A) Titration of Att-1-SFGFP plasmid. Fluorescence curves for plasmid concentrations 0.25, 0.5, and 1.0 nM. 0.5 nM was chosen for all further experiments. Shaded regions represent standard deviations of four independent reactions calculated at each time point. (B) – (D) SFGFP production rate curves used to calculate average SFGFP production rates in Figure 2D. Shaded regions represent standard deviations from at least seven independent reactions calculated at each time point. Boxes indicate regions of constant maximum SFGFP production used to calculate averages. (E) Titration of L2 of the transcription cascade in Figure 2E. L1 was held constant at 0.5 nM, while L2 varied between 4 and 8 nM. Average SFGFP production rates are shown with error bars representing standard deviations from four independent reactions. Total DNA concentration was kept at 8.5 nM across all reactions by adding additional no-antisense control DNA. 4 nM of L2 was chosen for all further experiments. (F) Titration of L3 of the transcription cascade in Figure 2E. L1 was held constant at 0.5 nM, L2 at 4 nM, and L3 varied from 10 – 18 nM. Average GFP production rates are shown with error bars representing standard deviations from four independent reactions. Total DNA concentration was kept at 22.5 nM across all reactions by adding additional no-antisense control DNA. 14 nM of L3 was chosen for all further experiments. Att-1: pT181 attenuator; AS-1: pT181 antisense; Att-2: pT181 mutant attenuator; AS-2: pT181 mutant antisense.

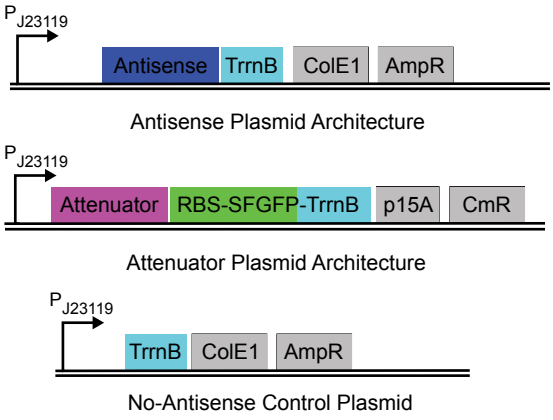

Figure S3. Plasmid architecture for attenuator and antisense plasmids. Antisense plasmids have the ColE1 origin and ampicillin resistance (AmpR). Attenuator plasmids have the p15A origin and chloramphenicol resistance (CmR). The J23119 *E. coli* consensus promoter (http://partsregistry.org/Part:BBa_J23119), modified to include a SpeI site right before the start of transcription, was used for all plasmids. TrrnB is a transcriptional terminator. RBS = ribosome binding site; SFGFP = super folder green fluorescent protein coding sequence. See Table S3 for sequence details of these plasmids.

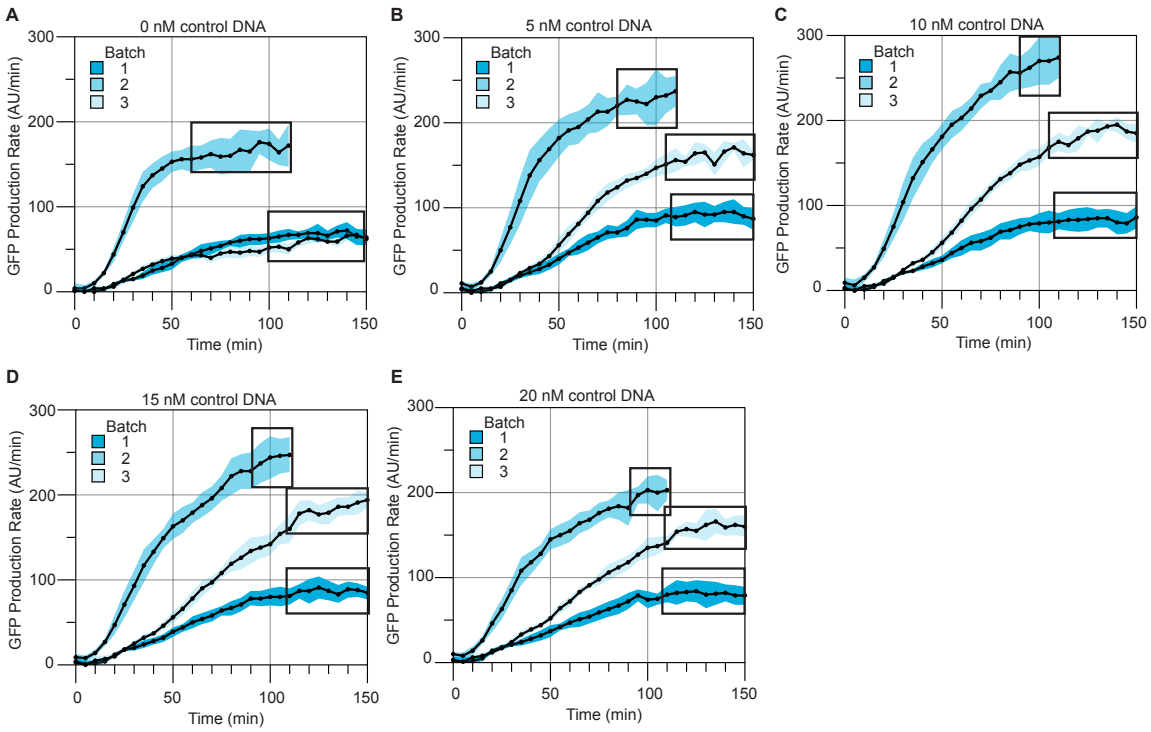

Figure S4. GFP production rate plots used to calculate the average GFP production in Figure 3B. 0.5 nM of L1 and the indicated concentration of no-antisense control DNA (0-20 nM) was tested with three extract and buffer batches. Shaded regions represent standard deviations from at least 11 independent reactions calculated at each time point.

Boxes represent constant maximum SFGFP production regions used to calculate averages. Batch 2 reached constant GFP production faster than batches 1 and 3, therefore data was only collected for 2 h for this batch.

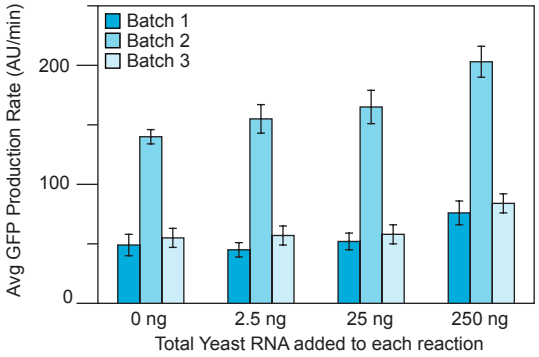

Figure S5. Addition of total yeast RNA to further assess batch-to-batch variation. Average maximum SFGFP production rates are reported for TX-TL reactions with 0.5 nM L1 and 0, 2.5, 25, and 250 ng of total yeast RNA. Error bars represent standard deviations of at least three independent reactions.

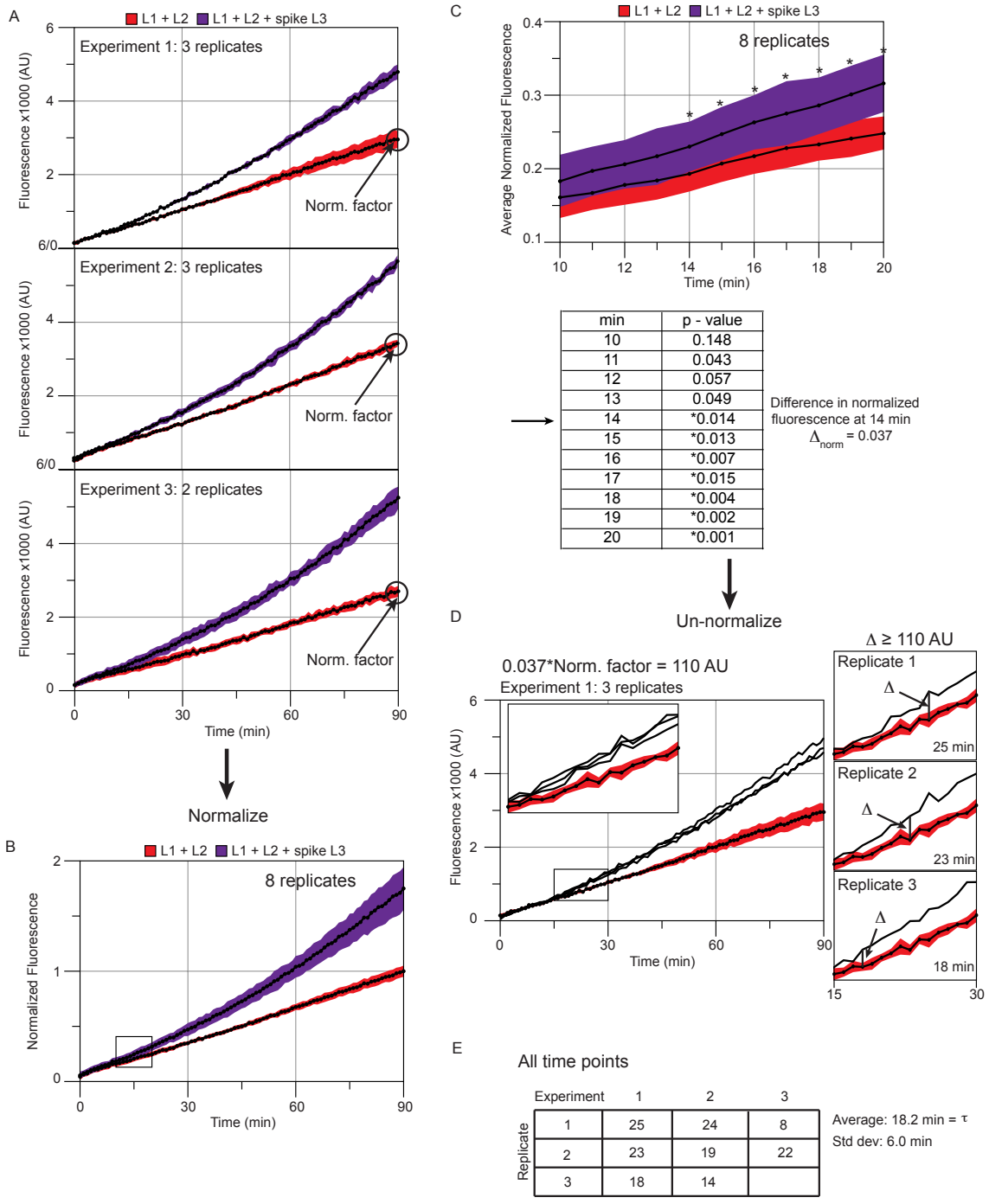

Figure S6. Calculation of circuit response time, τ. (See "Response Time Calculation" in **Methods**). (A) For the DNA spike experiments, three independent experiments were done with four replicates per experiment. Data was thrown out if a bubble was introduced into the well during addition of DNA. Averages (black line) plus and minus the standard deviation (shaded areas) are plotted within each experiment. (B) The average endpoint fluorescence of the L1+L2 curves in (A) were used to normalize all data points within an experiment. This allowed for all data points to be combined in a single

normalized fluorescence plot. Black lines indicated averages and shaded regions plus/minus standard deviations over the normalized trajectories. (C) For each time point, a Welch's t-test was used to determine whether the L1+L2 and L1+L2+L3 distributions over the normalized experimental replicates were statistically different from each other. The plot shows a zoomed-in region from (B). The * on the plot indicate times at which the t-test p-value was less than 0.05, with values listed in the table. The difference threshold, Δ_{norm}, in averaged normalized fluorescence was calculated at the earliest time where the two data sets were statistically different by this test. (D) For each experiment, the Δ_{norm} was converted into an un-normalized scale, Δ, by multiplying by the appropriate normalization factor. Each independent L1+L2+L3 trajectory was then compared to the average L1+L2 trajectory for that experiment to find the specific time at which the L1+L2+L3 trajectory was consistently greater than the average L1+L2 curve by Δ. These times are defined as the response time for that spike replicate. Example trajectories and response time depiction are shown for experiment 1. (E) Response times were calculated for all replicates and averaged to give the final τ value. A similar procedure was used to measure response times from *in vivo* experiments, with variations in the procedure noted in "Response Time Calculation" in **Methods**.

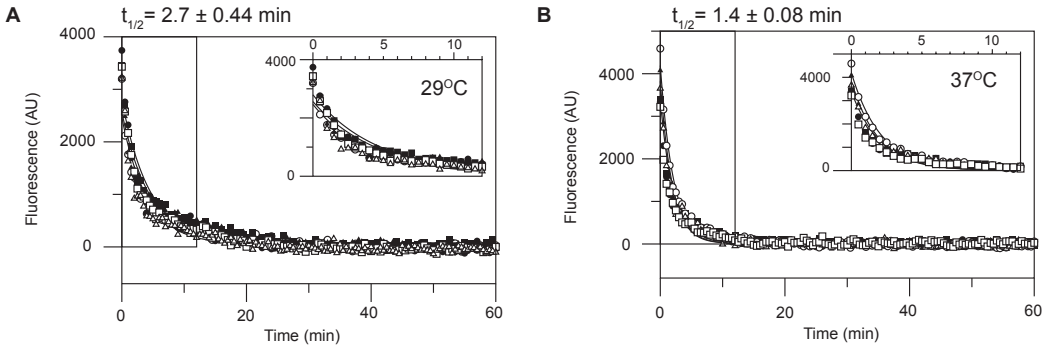

Figure S7. Degradation of the malachite green aptamer in TX-TL. Malachite green fluorescence trajectories taken at (A) 29°C and (B) 37°C for TX-TL batch 3 (Figure 3). 5.6 picomoles of aptamer was allowed to degrade in each reaction. Half lives ($t_{1/2}$) were calculated by fitting each trajectory to an exponential function of the form y(t) = a*exp(-t/τ) + b. τ values were used to calculate $t_{1/2}$. Error in $t_{1/2}$ represents standard deviations of six individual reactions. Inset plots magnify the initial fluorescence decay.

Table S1. Individual response times (τ) calculated for each experiment. All times reported in minutes.

Experiment	Individual τ values	Average ± Std dev	Figure
Att (DNA), 29°C	25, 23, 18, 24, 19, 14, 8, 22, 11	18.2 ± 6.0	4
Att (DNA), 37°C	17, 16, 23, 3, 18, 16, 14, 12, 14, 14, 14	14.6 ± 4.8	4
Att-Att (DNA), 37°C	19, 15, 25, 17, 14, 17, 28, 15, 25, 14, 25, 19	19.4 ± 5.0	5
Att (theophylline), 37°C	65, 58, 64, 54, 59, 47, 66, 56, 74, 61, 57, 51	59.3 ± 7.3	6
Att-Att (theophylline), 37°C	50, 41, 41, 37, 67, 35, 31, 46, 59	45.2 ± 11.7	6
SIM (*in vivo*), Att-Att-SFGFP	50, 40, 50, 30, 30, 30, 50, 30, 40, 30, 50, 50	40.0 ± 9.5	7
SIM (*in vivo*), Att-RFP	40, 50, 30, 30, 50, 60, 50, 10, 40, 40, 50, 50	41.7 ± 13.4	7
SIM (*in vivo*), Att-SFGFP	50, 50, 40, 50, 30, 30, 40, 20, 50, 50, 50, 50	42.5 ± 10.6	7
SIM (*in vivo*), Att-Att-RFP	60, 50, 50, 80, 50, 110, 90, 60, 90, 90, 70	72.7 ± 20.5	7

Table S2. P-values from Welch's t-test comparing response times from different experiments.

Experiment 1	Experiment 2	p-value	Figure
Att (DNA), 29°C	Att (DNA), 37°C	0.1694	4
Att (DNA), 37°C	Att-Att (DNA), 37°C	0.0303	4, 5

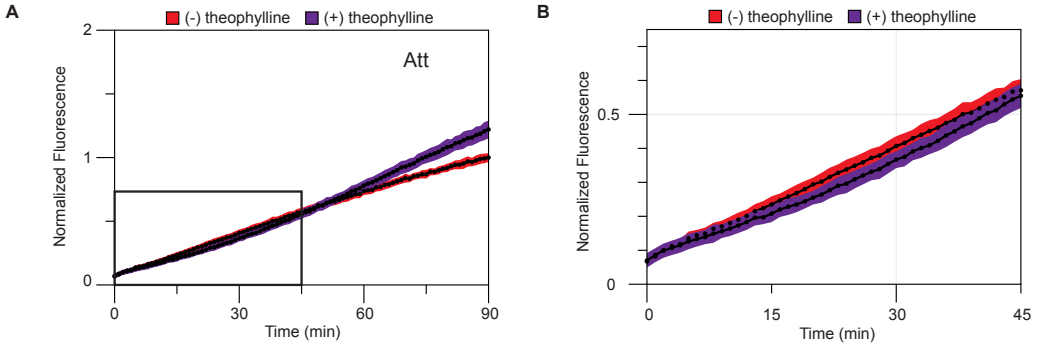

Figure S8. (A) Fluorescence trajectories from the theophylline responsive, single attenuator cascade in Figure 6B. (B) Magnified view of the fluorescence trajectories in A from 0 to 45 min to show the dip in the (+) theophylline curve.

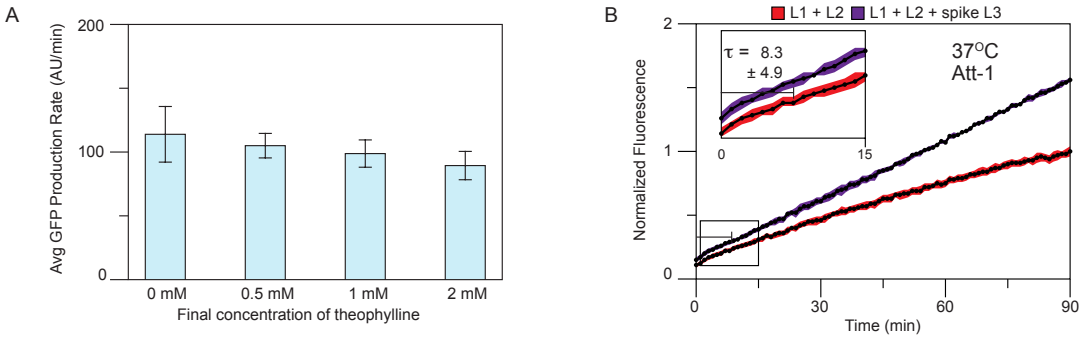

Figure S9. (A) Theophylline toxicity test in TX-TL. Average maximum SFGFP production rates are reported for TX-TL reactions with 0.5 nM L1 and 0, 0.5, 1, and 2 mM of theophylline. Error bars represent standard deviations of at least three independent reactions. (B) DNA spike experiment for the Att-1 cascade with added theophylline. The same experimental setup as in Figure 4C except that theophylline or water (as a control) was spiked in along with the L3 DNA. Normalized fluorescence curves from a single experiment performed at 37°C with a total of 4 replicates. τ = 8.3 ± 4.9 min. Shaded regions represent standard deviations calculated at each time point.

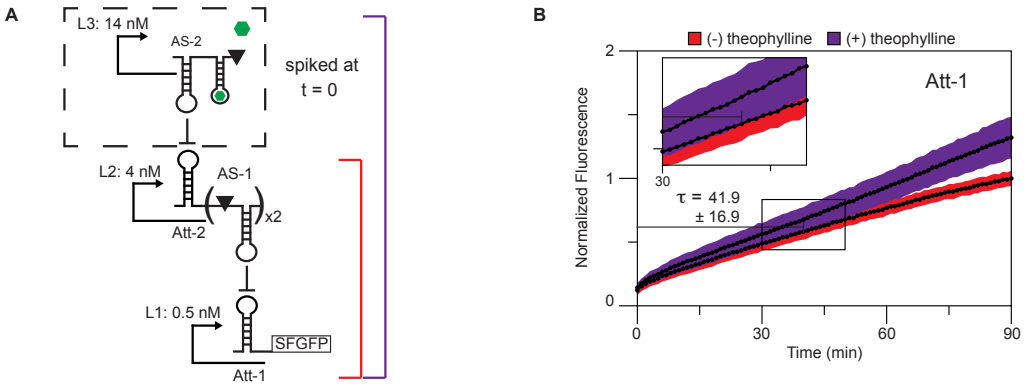

Figure S10. Theophylline and aptamer-AS-2 co-spike. (A) Schematic of a similar experiment to Figure 6B and Figure S9B, where aptamer-AS-2 with (+) and without (-) theophylline was spiked into an ongoing L1+L2 TX-TL reaction at t = 0. (B) Normalized fluorescence curves combining three separate experiments performed at 37°C with a total of 12 replicates over multiple days. τ = 41.9 ± 16.9 min. Shaded regions represent standard deviations calculated at each time point.

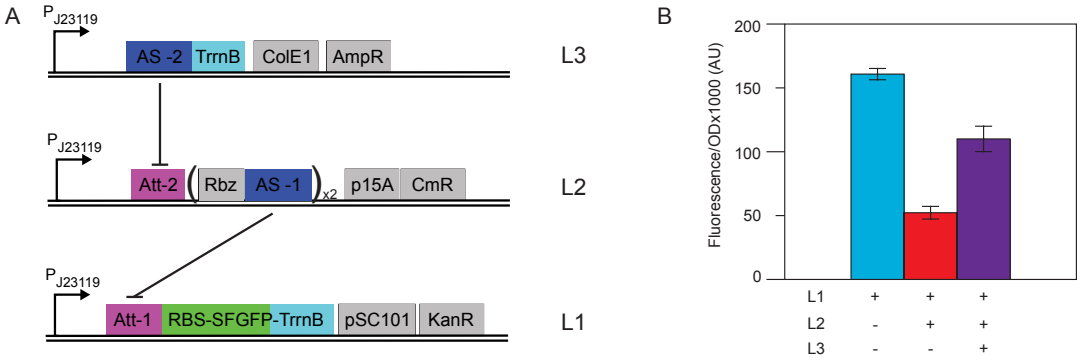

Figure S11. (A) Plasmid architecture for the 3-plasmid transcription cascade. L1 contains the pT181 attenuator (Att-1) upstream of the SFGFP coding sequence on a pSC101 backbone with kanamycin resistance. L2 contains the ribozyme-pT181 antisense (Rbz AS-1) controlled by the pT181 mutant attenuator (Att-2) on a p15A backbone with chloramphenicol resistance. L3 contains the pT181 mutant antisense (AS-2) on a ColE1 backbone with ampicillin resistance. See Table S3 for sequence details of these plasmids. (B) *In vivo* steady state expression data from cells co-transformed with L1 (blue bar), L1+L2 (red bar), or L1+L2+L3 (purple bar). Control plasmids lacking functional coding sequences were used in place of L2 and L3 for the (-) conditions. Error bars represent standard deviations of 4 independent transformants.

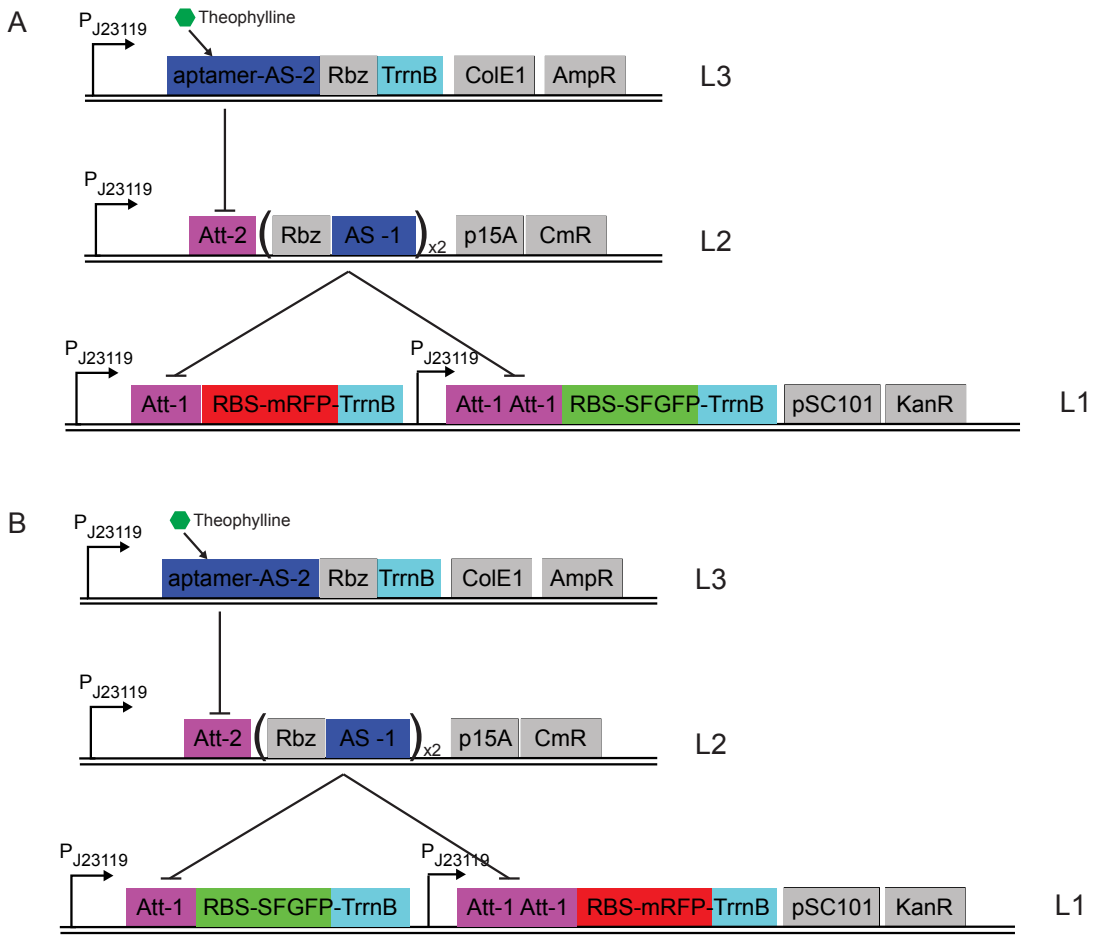

Figure S12. *In vivo* SIM plasmid architecture. (A) The bottom level (L1) contains both a single pT181 attenuator (Att-1) upstream of the RFP coding sequence and tandem pT181 attenuators (Att-1-Att-1) upstream of the SFGFP coding sequence on a pSC101 backbone with kanamycin resistance. L2 contains the pT181 antisense (AS-1) controlled by the pT181 mutant attenuator (Att-2) on a p15A backbone with chloramphenicol resistance. L3 contains the theophylline aptamer-pT181 mutant antisense fusion (aptamer-AS-2) on a ColE1 backbone with ampicillin resistance. (B) L2 and L3 are the same as in A. L1 contains Att-1 upstream of the SFGFP coding sequence and tandem Att-1-Att-1 upstream of the RFP coding sequence on a pSC101 backbone with kanamycin resistance. See Table S3 and S4 for sequence details of these plasmids.

Table S3: Important DNA sequences

Name	Sequence
pT181 attenuator (EcoRI-J23119-attenuator)	GAATTCTAAAGATCTTTGACAGCTAGCTCAGTCCTAGGTATAATACTAGTAACA AAATAAAAAGGAGTCGCTCACGCCCTGACCAAAGTTTGTGAACGACATCATTC AAAGAAAAAAACACTGAGTTGTTTTTATAATCTTGTATATTTAGATATTAAACGA TATTTAAATATACATAAAGATATATATTTGGGTGAGCGATTCCTTAAACGAAATT GAGATTAAGGAGTCGCTCTTTTTTATGTATAAAAACAATCATGCAAATCATTCA AATCATTTGGAAAATCACGATTTAGACAATTTTTCTAAAACCGGCTACTCTAAT AGCCGGTTGTAAGGATCT
pT181-mutant	GAATTCTAAAGATCTTTGACAGCTAGCTCAGTCCTAGGTATAATACTAGTAACA AAATAAAAAGGAGTCGCTCTGTCCCTCGCCAAAGTTGCAGAACGACATCATTC

attenuator (EcoRI-J23119-attenuator)	AAAGAAAAAAACACTGAGTTGTTTTTATAATCTTGTATATTTAGATATTAAACGA TATTTAAATATACATAAAGATATATATTTGGGTGAGCGATTCCTTAAACGAAATT GAGATTAAGGAGTCGCTCTTTTTTATGTATAAAAACAATCATGCAAATCATTCA AATCATTTGGAAAATCACGATTTAGACAATTTTTCTAAAACCGGCTACTCTAAT AGCCGGTTGTAAGGATCT
Super folder green fluorescent protein (Ribosome binding site - SFGFP)	AGGAGGAAGGATCTATGAGCAAAGGAGAAGAACTTTTCACTGGAGTTGTCCC AATTCTTGTTGAATTAGATGGTGATGTTAATGGGCACAAATTTTCTGTCCGTGG AGAGGGTGAAGGTGATGCTACAAACGGAAAACTCACCCTTAAATTTATTTGCA CTACTGGAAAACTACCTGTTCCGTGGCCAACACTTGTCACTACTCTGACCTAT GGTGTTCAATGCTTTTCCCGTTATCCGGATCACATGAAACGGCATGACTTTTT CAAGAGTGCCATGCCCGAAGGTTATGTACAGGAACGCACTATATCTTTCAAAG ATGACGGGACCTACAAGACGCGTGCTGAAGTCAAGTTTGAAGGTGATACCCT TGTTAATCGTATCGAGTTAAAGGGTATTGATTTTAAAGAAGATGGAAACATTCT TGGACACAAACTCGAGTACAACTTTAACTCACACAATGTATACATCACGGCAG ACAAACAAAAGAATGGAATCAAAGCTAACTTCAAAATTCGCCACAACGTTGAA GATGGTTCCGTTCAACTAGCAGACCATTATCAACAAAATACTCCAATTGGCGA TGGCCCTGTCCTTTTACCAGACAACCATTACCTGTCGACACAATCTGTCCTTT CGAAAGATCCCAACGAAAAGCGTGACCACATGGTCCTTCTTGAGTTTGTAACT GCTGCTGGGATTACACATGGCATGGATGAGCTCTACAAATAA
TrrnB	GAAGCTTGGGCCCGAACAAAAACTCATCTCAGAAGAGGATCTGAATAGCGCC GTCGACCATCATCATCATCATCATTGAGTTTAAACGGTCTCCAGCTTGGCTGT TTTGGCGGATGAGAGAAGATTTTCAGCCTGATACAGATTAAATCAGAACGCAG AAGCGGTCTGATAAAACAGAATTTGCCTGGCGGCAGTAGCGCGGTGGTCCCA CCTGACCCCATGCCGAACTCAGAAGTGAAACGCCGTAGCGCCGATGGTAGTG TGGGGTCTCCCCATGCGAGAGTAGGGAACTGCCAGGCATCAAATAAAACGAA AGGCTCAGTCGAAAGACTGGGCCTTTCGTTTTATCTGTTGTTTGTCGGTGAAC T
Monomeric red fluorescent protein (Ribosome binding site-mRFP)	ACAGTCGATGGCAAGTAGCGAAGACGTTATCAAAGAGTTCATGCGTTTCAAAG TTCGTATGGAAGGTTCCGTTAACGGTCACGAGTTCGAAATCGAAGGTGAAGG TGAAGGTCGTCCGTACGAAGGTACCCAGACCGCTAAACTGAAAGTTACCAAA GGTGGTCCGCTGCCGTTCGCTTGGGACATCCTGTCCCCGCAGTTCCAGTACG GTTCCAAAGCTTACGTTAAACACCCGGCTGACATCCCGGACTACCTGAAACTG TCCTTCCCGGAAGGTTTCAAATGGGAACGTGTTATGAACTTCGAAGACGGTG GTGTTGTTACCGTTACCCAGGACTCCTCCCTGCAAGACGGTGAGTTCATCTAC AAAGTTAAACTGCGTGGTACCAACTTCCCGTCCGACGGTCCGGTTATGCAGA AAAAAACCATGGGTTGGGAAGCTTCCACCGAACGTATGTACCCGGAAGACGG TGCTCTGAAAGGTGAAATCAAAATGCGTCTGAAACTGAAAGACGGTGGTCACT ACGACGCTGAAGTTAAAACCACCTACATGGCTAAAAAACCGGTTCAGCTGCC GGGTGCTTACAAAACCGACATCAAACTGGACATCACCTCCCACAACGAAGAC TACACCATCGTTGAACAGTACGAACGTGCTGAAGGTCGTCACTCCACCGGTG CTTAATAA
pT181 antisense (EcoRI-J23119-antisense)	GAATTCTAAAGATCTTTGACAGCTAGCTCAGTCCTAGGTATAATACTAGTATAC AAGATTATAAAAACAACTCAGTGTTTTTTTCTTTGAATGATGTCGTTCACAAACT TTGGTCAGGGCGTGAGCGACTCCTTTTTATTTGGATCT
pT181 mutant antisense (EcoRI-J23119-antisense)	GAATTCTAAAGATCTTTGACAGCTAGCTCAGTCCTAGGTATAATACTAGTATAC AAGATTATAAAAACAACTCAGTGTTTTTTTCTTTGAATGATGTCGTTCTGCAACT TTGGCGAGGGACAGAGCGACTCCTTTTTATTTGGATCT
Theophylline aptamer-pT181-mutant	GGTGATACCAGCATCGTCTTGATGCCCTTGGCAGCACCTCTTTGAATGGTGCT GCCCTGCAACTTTGGCGAGGGACAGGGCGACTCCTTTTTATTTCTGTCACCG GATGTGCTTTCCGGTCTGATGAGTCCGTGAGGACGAAACAG

antisense (aptamer-antisense-sTRSV Ribozyme)	
sTRSV Ribozyme	CTGTCACCGGATGTGCTTTCCGGTCTGATGAGTCCGTGAGGACGAAACAG
Tandem pT181 attenuators(J23119-attenuator-XhoI-attenuator)	TTGACAGCTAGCTCAGTCCTAGGTATAATACTAGTAACAAAATAAAAAGGAGT CGCTCACGCCCTGACCAAAGTTTGTGAACGACATCATTCAAAGAAAAAAACAC TGAGTTGTTTTTATAATCTTGTATATTTAGATATTAAACGATATTTAAATATACAT AAAGATATATATTTGGGTGAGCGATTCCTTAAACGAAATTGAGATTAAGGAGT CGCTCTTTTTTATGTATAAAAACAATCATGCAAATCATTCAAATCATTTGGAAAA TCACGATTTAGACAATTTTTCTAAAACCGGCTACTCTAATAGCCGGTTGTAACT CGAGAACAAAATAAAAAGGAGTCGCTCTGTCCCTCGCCAAAGTTGCAGAACG ACATCATTCAAAGAAAAAAACACTGAGTTGTTTTTATAATCTTGTATATTTAGAT ATTAAACGATATTTAAATATACATAAAGATATATATTTGGGTGAGCGATTCCTTA AACGAAATTGAGATTAAGGAGTCGCTCTTTTTTATGTATAAAAACAATCATGCA AATCATTCAAATCATTTGGAAAATCACGATTTAGACAATTTTTCTAAAACCGGC TACTCTAATAGCCGGTTGTAAGGATCT
Double pT181 antisense (BamHI-BglII Scar-sTRSV Ribozyme antisense)x2	GGATCTCTGTCACCGGATGTGCTTTCCGGTCTGATGAGTCCGTGAGGACGAA ACAGGGATCTATACAAGATTATAAAAACAACTCAGTGTTTTTTTCTTTGAATGA TGTCGTTCACAAACTTTGGTCAGGGCGTGAGCGACTCCTTTTTATTTGGATCT CTGTCACCGGATGTGCTTTCCGGTCTGATGAGTCCGTGAGGACGAAACAGGG ATCCTAACTCGAGATACAAGATTATAAAAACAACTCAGTGTTTTTTTCTTTGAAT GATGTCGTTCACAAACTTTGGTCAGGGCGTGAGCGACTCCTTTTTATTTGGAT CT

Table S4 – Plasmids used in this study. Sequences in the plasmid architecture (Figures S3, S11, S12) can be found in Table S3.

Plasmid #	Plasmid architecture	Name	Figure
JBL006	J23119 – pT181 attenuator – SFGFP – TrrnB – CmR – p15A origin	pT181 attenuator, Att-1	2, 3, 4, 5, 6, S2, S4, S5, S6, S8, S9, S10
JBL004	J23119 – pT181 antisense – TrrnB – ColE1 origin – AmpR	pT181 antisense, AS-1	2, S2
JBL002	J23119 – TrrnB – ColE1 origin – AmpR	No antisense control	2, 3, 4, 5, S2, S4, S6, S11
JBL007	J23119 – pT181 mutant attenuator – SFGFP – TrrnB – CmR – p15A origin	pT181 mutant attenuator, Att-2	2, S2
JBL008	J23119 – pT181 mutant antisense – TrrnB – ColE1 origin – AmpR	pT181 mutant antisense, AS-2	2, 4, 5, S2, S6, S11
JBL069	J23119 – pT181 mutant attenuator – (sTRSV ribozyme – pT181 antisense)x2 – TrrnB – ColE1 origin – AmpR	Cascade L2	2, 4, 5, 6, S2,

			S6, S8, S9, S10
JBL015	J23119 – (pT181 attenuator)x2 – SFGFP – TrrnB – CmR – p15A origin	Tandem pT181 attenuators, Att-1-Att-1	5, 6
JBL1843	J23119 – theophylline aptamer-pT181 mutant antisense – sTRSV ribozyme – TrrnB – ColE1 origin – AmpR	Aptamer pT181 mutant antisense, aptamer-AS-2	6, 7, S8, S10
JBL1852	J23119 – pT181 attenuator – mRFP – TrrnB – J23119 – (pT181 attenuator)x2 – SFGFP – TrrnB – pSC101 origin – KanR	SIM L1	7
JBL1853	J23119 – pT181 attenuator – SFGFP – TrrnB – J23119 – (pT181 attenuator)x2 – mRFP – TrrnB – pSC101 origin – KanR	SIM L1 (switch)	7
JBL1844	J23119 – pT181 mutant attenuator – (sTRSV ribozyme – pT181 antisense)x2 – TrrnB – CmR – p15A origin	Cascade L2 on p15A/CmR backbone	7, S11
JBL1855	J23119 – pT181 attenuator – SFGFP – TrrnB – pSC101 origin – KanR	pT181 attenuator	S11
JBL1856	TrrnB – pSC101 origin – KanR	pSC101/KanR control	S11
JBL001	TrrnB – CmR – p15A origin	CmR/p15A control	S11

References

(1) Sun, Z. Z., Hayes, C. A., Shin, J., Caschera, F., Murray, R. M., and Noireaux, V. (2013) Protocols for Implementing an Escherichia coli Based TX-TL Cell-Free Expression System for Synthetic Biology. *Journal of Visualized Experiments* 70, e50762.
(2) Novick, R. P., Iordanescu, S., Projan, S. J., Kornblum, J., and Edelman, I. (1989) pT181 plasmid replication is regulated by a countertranscript-driven transcriptional attenuator. *Cell 59*, 395–404.
(3) Brantl, S., and Wagner, E. G. (2000) Antisense RNA-mediated transcriptional attenuation: an in vitro study of plasmid pT181. *Mol Microbiol 35*, 1469–1482.
(4) Takahashi, M. K., and Lucks, J. B. (2013) A modular strategy for engineering orthogonal chimeric RNA transcription regulators. *Nucleic acids research 41*, 7577–7588.

APPENDIX 1: ESTIMATION OF THE RESPONSE TIME OF A DOUBLE-INVERSION RNA CASCADE

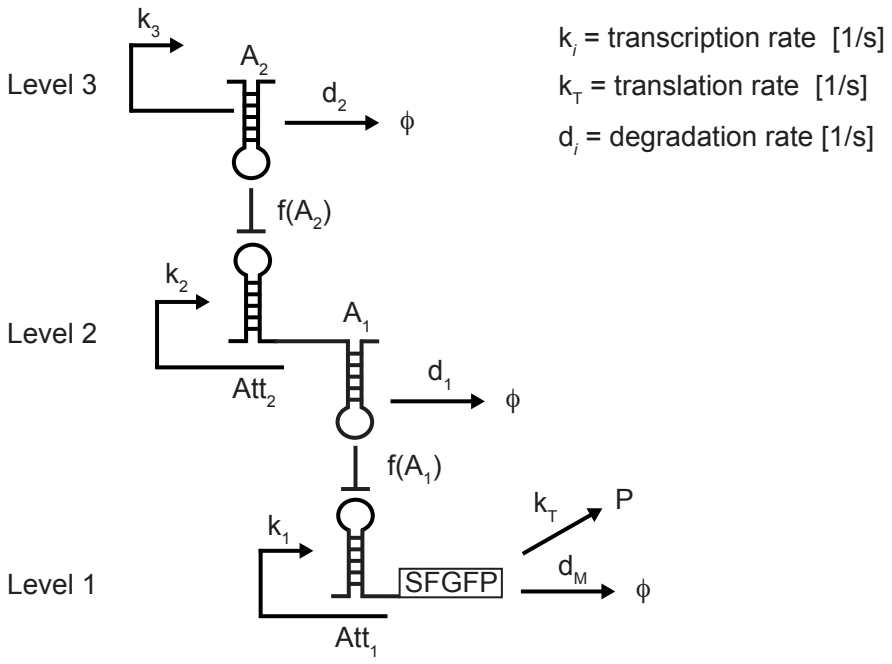

FIGURE 1. A double inversion RNA cascade. The cascade consists of three levels, transcribed from three separate pieces of DNA. Antisense molecules (A_i) interact with attenuator sequences (Att_i) to suppress the transcription of the sequence downstream of the attenuator. Numbers indicate pairs of antisense-attenuator, which are assumed to be perfectly orthogonal to each other (i.e. A_1 only targets Att_1, etc.). $f(A_i)$ relates how much of the downstream sequence is transcribed versus A_i concentration. Key parameters of the model are indicated.

We consider the double inversion RNA transcriptional cascade depicted in Figure (1). In the simplest model, we can calculate the dynamical behavior of this network using ordinary differential equations that capture the basic chemical reactions of gene expression at each level of the cascade ([1]).

$$\frac{\mathrm{d}A_2}{\mathrm{d}t}(t) = k_3 - d_2 A_2(t), \tag{1}$$

$$\frac{\mathrm{d}A_1}{\mathrm{d}t}(t) = k_2 f(A_2(t)) - d_1 A_1(t), \tag{2}$$

$$\frac{\mathrm{d}M}{\mathrm{d}t}(t) = k_1 f(A_1(t)) - d_M M(t), \tag{3}$$

$$\frac{\mathrm{d}P}{\mathrm{d}t}(t) = k_T M(t). \tag{4}$$

Here A_i represents the concentration of the antisense signal species, and M and P denote the concentrations of mRNA and protein, respectively, of the experimentally observable fluorescent protein encoded in the first level of the cascade. We have also used the approximation that P does not degrade on the timescale of a TX-TL experiment and therefore has no degradation term. Since these equations represent number of molecules, k_i and d_i have units of $1/s$.

Note that since this is an RNA circuit, we only need to consider translation of the final reporter level - each of the intermediate levels of the cascade can be described by a single equation representing the transcription and degradation dynamics of the RNA species. We are also ignoring additional effects due to the ribozyme in level 2 that is present in the real cascade (Figure 2E of the main text.)

Our goal is to estimate the response time of this network to a spike in the concentration of the level 3 DNA at time $t = 0$. To calculate this estimate, we make the simplifying assumption of a threshold function for $f(A)$, following ([1]). Under this assumption $f(x \geq \beta) = 0$, and $f(x < \beta) = 1$ as depicted in Figure (2), for some threshold β. Under this assumption, an antisense species will completely repress the transcription of its target when its concentration is above β.

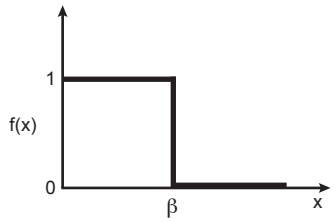

FIGURE 2. The f function is taken to be a step function with threshold β.

To model the spike experiment, we consider the initial condition

$$A_2(t \leq 0) = 0. \tag{5}$$

We also assume that the reactions have been proceeding long enough before $t = 0$ for A_1 to have reached steady-state, i.e.

$$A_1(t = 0) = \frac{k_2}{d_1}, \tag{6}$$

which uses eq. (5), and our threshold assumption.

We now solve each equation in turn: Using the initial condition eq. (5), and an integration factor, we find

$$A_2(t) = \frac{k_3}{d_2}(1 - e^{-d_2 t}). \tag{7}$$

Solving for $A_1(t)$ is made easier by considering the time, δ_2, at which $A_2(t)$ reaches the threshold needed to attenuate the transcription of A_1, which we label β_2 (see Figure 5A of the main text). Solving $A_2(\delta_2) = \beta_2$ gives

$$\delta_2 = \frac{1}{d_2} \ln\left(\frac{k_3/d_2}{k_3/d_2 - \beta_2}\right). \tag{8}$$

Using an integrating factor to solve for $A_1(t)$, we find

$$A_1(t) = A_1(0)e^{-d_1 t} + k_2 e^{-d_1 t} \int_0^t f(A_2(t'))e^{d_1 t'} \mathrm{d}t'. \tag{9}$$

Using the threshold function, the last integral can be taken from $t = 0$ to $t = \delta_2$, and plugging in the steady state condition for $A_1(0)$ from eq. (6), we find

$$A_1(t) = \frac{k_2}{d_1} e^{-d_1(t-\delta_2)}. \tag{10}$$

Similarly, to solve for $M(t)$, we first find the time, δ_1, at which $A_1(t)$ reaches the threshold needed to attenuate the transcription of M, which we label β_1. Solving $A_1(\delta_1) = \beta_1$ gives

$$\delta_1 = \delta_2 + \frac{1}{d_1} \ln\left(\frac{k_2/d_1}{\beta_1}\right). \tag{11}$$

Using an integrating factor to solve for $M(t)$, we find

$$M(t) = e^{-d_M t}\left(M(0) + k_1 \int_0^t f(A_1(t'))e^{d_M t'} \mathrm{d}t'\right). \tag{12}$$

We assume that initially $A_1(0) > \beta_1$ so that $f(A_1(t < \delta_1)) = 0$ and M is initially not expressed. This also means $M(0) = 0$ by our threshold assumption. When $t \geq \delta_1$, then $A_1(t) < \beta_1$ and $M(t)$ can be expressed. Using this, we find

$$M(t) = \begin{cases} 0, & t < \delta_1, \\ \frac{k_1}{d_M}\left(1 - e^{-d_M(t-\delta_1)}\right), & t \geq \delta_1. \end{cases} \tag{13}$$

We note that the extra steps of the circuitry effectively delay the response of M transcription by a time δ_1.

In a similar manner we can solve for $P(t)$, using the fact that $P(t < \delta_1) = 0$:

$$P(t) = k_T \int_0^t M(t')\mathrm{d}t' = k_T \int_{\delta_1}^t M(t')\mathrm{d}t', \tag{14}$$

which when we use eq. (13) we find

$$P(t) = \begin{cases} 0, & t < \delta_1, \\ \frac{k_T k_1}{d_M} \left((t - \delta_1) - \frac{1}{d_M}(1 - e^{-d_M(t-\delta_1)} \right), & t \geq \delta_1. \end{cases} \tag{15}$$

Since the protein must go through a maturation step before it can be observed, characterized by a time α, we find that the circuit response time, $\tau = \delta_1 + \alpha$, to be

$$\tau = \frac{1}{d_2} \ln \left(\frac{k_3/d_2}{k_3/d_2 - \beta_2} \right) + \frac{1}{d_1} \ln \left(\frac{k_2/d_1}{\beta_1} \right) + \alpha. \tag{16}$$

A reasonable estimate for the threshold values is one half of the steady-state concentration of each species, or $\beta_2 \sim \frac{1}{2}\frac{k_3}{d_2}$ and $\beta_1 \sim \frac{1}{2}\frac{k_2}{d_1}$, which gives

$$\tau \sim \ln(2) \left(\frac{1}{d_2} + \frac{1}{d_1} \right) + \alpha. \tag{17}$$

For the tandem attenuator, by the multiplication rule ([2]), we assume $\beta_1' \sim \frac{1}{4}\frac{k_2}{d_1}$, so find

$$\tau' \sim \ln(2)\frac{1}{d_2} + \ln(4)\frac{1}{d_1} + \alpha. \tag{18}$$

Figure 5A in the text shows a graphical representation of these results.

References

[1] Alon U (2007) *An Introduction to Systems Biology: Design Principles of Biological Circuits.* Chapman and Hall/CRC, Boca Raton, Fl.

[2] Lucks JB, Qi L, Mutalik VK, Wang D, Arkin AP (2011) Versatile RNA-sensing transcriptional regulators for engineering genetic networks. *PNAS* 108:8617-8622.